

# Chapter 7

## Biogeography of Triassic Ammonoids

Arnaud Brayard, Gilles Escarguel, Claude Monnet,  
James F. Jenks and Hugo Bucher

### 7.1 Introduction

Ammonoids nearly died out during the Permian-Triassic (PT) mass extinction (~252 Ma), but quickly and rather impressively recovered in less than ~1.5 myr during the Early Triassic (Tozer 1981a; Brayard et al. 2009a; Brayard and Bucher 2015; Fig. 7.1). Only one survivor group, a derivative of the Xenodiscaceae, is usually considered as the root-stock of all Triassic, and thus, all post-Triassic ammonoids (Kummel 1973a; Spinosa et al. 1975; Tozer 1981a, 1981b; Page 1996; Brayard et al. 2006), making post-PT ammonoids a “quasi-monophyletic” group (but see Kummel 1972; Glenister and Furnish 1981; Brayard et al. 2007a; McGowan and Smith 2007; Leonova 2011; Zakharov and Moussavi Abnavi 2013). The Triassic

---

A. Brayard (✉)

UMR CNRS 6282 Biogéosciences, Université de Bourgogne, 21000 Dijon,  
6 boulevard Gabriel, France  
e-mail: arnaud.brayard@u-bourgogne.fr

G. Escarguel

UMR CNRS 5276, Laboratoire de Géologie de Lyon: Terre, Planètes, Environnement,  
Université Claude Bernard Lyon 1, 27–43 Boulevard du 11 novembre 1918,  
69622 Villeurbanne Cedex, France  
e-mail: gilles.escarguel@univ-lyon1.fr

C. Monnet

UMR CNRS 8217 Géosystèmes, UFR des Sciences de la Terre—Bât. SN5,  
Université de Lille 1, Avenue Paul Langevin, 59655 Villeneuve d’Ascq cedex, France  
e-mail: claudemonnet@univ-lille1.fr

J. F. Jenks

1134 Johnson Ridge Lane, 84084 West Jordan, UT, USA  
e-mail: jenksjimruby@gmail.com

H. Bucher

Paläontologisches Institut und Museum, Universität Zürich,  
Karl-Schmid Strasse 4, 8006 Zürich, Switzerland  
e-mail: hugo.fr.bucher@pim.uzh.ch

© Springer Science+Business Media Dordrecht 2015

C. Klug et al. (eds.), *Ammonoid Paleobiology: From macroevolution to paleogeography*,  
Topics in Geobiology 44, DOI 10.1007/978-94-017-9633-0\_7

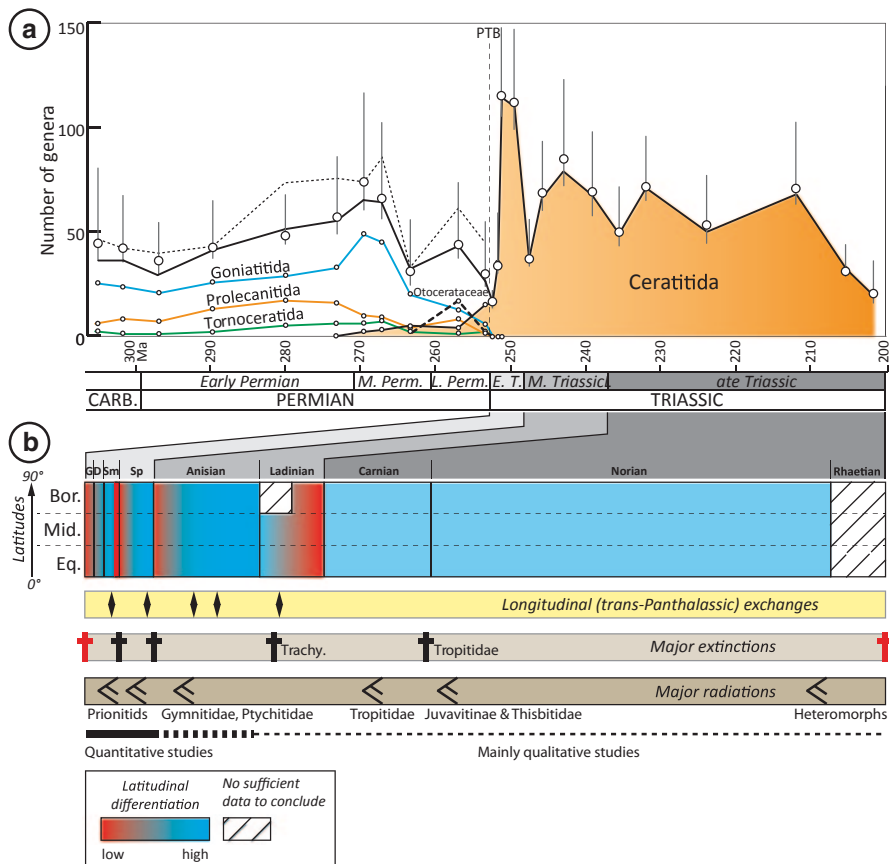


**Fig. 7.1** **a** Total generic richness (*black bold line*: all ammonoids; *colored lines*: major ammonoid groups; *Permian bold line*: data from Goniat.org; *Permian dotted line*: alternate data from the AMMON database (Korn and Ilg 2007); *Triassic bold line* modified after Brayard et al. (2009a) based on an updated database) and mean Chao2 estimate of the overall generic richness with its 95% Confidence Interval (*large circles* with vertical bars). *PTB* Permo-Triassic boundary. *E.T.* Early Triassic. Note that the end-Smithian ammonoid extinction event discussed in the text is not illustrated here due to its short time duration. **b** Present well-known biogeographical and evolutionary patterns. *Bor.* Boreal, *Mid.* Middle, *Eq.* Equatorial

remains one of the most interesting and intriguing periods for ammonoid evolution as it is marked by successive episodes of intense radiation and marked extinction associated with sudden biogeographic changes often closely related to major climatic and oceanographic changes (e.g. Tozer 1982; Dagys 1988; Dagys and Ermakova 1990; Brayard et al. 2006, 2007b, 2009a, c; Monnet and Bucher 2006a; Galfetti et al. 2007a; Konstantinov 2008; Zakharov et al. 2008; Balini et al. 2010; Monnet et al. 2013; Zakharov and Moussavi Abnavi 2013). The end of the Triassic is also marked by the enigmatic appearance of the first heteromorphs and a further near-annihilation at the Triassic/Jurassic boundary (~201 Ma).

Ammonoid diversity and disparity patterns are now well-known globally and certain restricted Triassic intervals have been intensively studied (e.g. for the Early

Triassic: McGowan 2004, 2005; Brayard et al. 2007b, 2009c; Brosse et al. 2013). However, until recently, the biogeographical trends of Middle and Late Triassic ammonoids for the most part were only superficially investigated, and the same is true for their potential underlying processes (Kummel 1973b; Tozer 1981a, 1981b, 1982; Dagys 1988; Page 1996; Fig. 7.1). Indeed, they most often were based only on qualitative comparisons between uneven geographic areas (e.g. from local outcrops to global realms, according to the author's subjectivity) or between distinct taxonomic groups. Previous biogeographic studies of Triassic ammonoids were not often focused on a specific time-interval and were rarely based on quantitative methods (but see Kummel and Steele 1962 for a noticeable exception).

Significant biogeographic progress has been made recently with regard to the use of quantitative methods on large datasets combined with computer modeling (Brayard et al. 2004, 2006, 2007b, 2009c). These large datasets benefited from the infusion of much new primary data generated by intensive fieldwork and carefully-revised taxonomy (e.g. Monnet and Bucher 2005; Jenks 2007; Brayard and Bucher 2008; Shigeta and Zakharov 2009; Guex et al. 2010; Jenks et al. 2010; Ware et al. 2011; Balini et al. 2012a, 2012b; Brühwiler et al. 2012a, 2012b, 2012c; Brayard et al. 2013; Zakharov and Moussavi Abnavi 2013) occasionally combined with recently-published radiometric ages (e.g. Galfetti et al. 2007a; Schaltegger et al. 2008). This chapter emphasizes these quantitative methods and inferred relationships between ammonoid biogeographical changes during the Triassic and potential controlling factors such as gradients of Sea Surface Temperature (SST) and oceanic circulation. The biostratigraphic framework used in the following discussion is detailed in the chapter "Triassic biostratigraphy" (Jenks et al. 2015).

## 7.2 What's New in Triassic Ammonoid Macroecological and Biogeographical Analyses?

### 7.2.1 *Classical Analyses and Explored Patterns*

The vast majority of studies of past and present-day global diversity have demonstrated the existence of pervasive geographic patterns such as a Pole-to-Equator gradient, both on land and sea (e.g. Stehli et al. 1969; Gaston 2000; Powell 2007). Others have shown for instance, different large-scale patterns in longitude (e.g. Connolly et al. 2003), altitude (e.g. McCain 2004), bathymetry (e.g. Pineda and Caswell 1998), endemism (e.g. Gaston 1994), range size (Gaston 2003), or size of organisms (e.g. Roy et al. 2001; Zhang and Payne 2012). However, the processes explaining the edification of such large-scale patterns, and especially the latitudinal diversity gradient, are still a matter of debates (e.g. Brayard et al. 2005; Colwell et al. 2005; Jablonski et al. 2006; Escarguel et al. 2008; Beaugrand et al. 2013). One of the core questions remains the very existence and overall importance of deterministic (functional) drivers over historical contingency in generating and controlling such macroecological patterns. Because evolutionary time is a dimension lacking in

neontological studies, fossil-based deep-time analyses can greatly improve the knowledge and understanding of the edification of these large-scale patterns.

Ammonoids are generally well-suited for such analyses due to their widespread geographical distribution and high evolutionary rates. Most diversity and biogeographic studies are based on taxonomic count and geographic occurrences because these measures are (i) the simplest to acquire, (ii) expected to be the most robust to sampling biases, and (iii) less arbitrary in their definition and measurements. Temporal dynamics in richness and evolutionary rate changes in ammonoids are customarily represented as curves based on the succession of studied time bins. As these analyses often compare intervals with different duration, sampling intensity, paleoenvironments or geographic scales, their results may not be directly comparable, if not intrinsically biased. However, some of these biases can be controlled, if not at least partly ruled out, using for instance traditional sample-based rarefaction curves (Foote 1992; Dommergues et al. 2009) in order to compare the taxonomic diversity estimates at comparable levels of sampling effort. Other potential bias such as the unequal duration of time bins, from which diversity counts are obtained, can be circumvented by the use of Unitary Association Zones. These have been demonstrated to be largely immune to this problem (Escarguel and Bucher 2004).

Regarding ammonoid biogeographical structuring, quantitative large-scale analyses remain rather uncommon and are defined at different time-scales and taxonomic levels according to the available data (e.g. McGowan 2005; Brayard et al. 2006, 2007b, 2009c; Dommergues et al. 2009; Dera et al. 2011; Korn et al. 2012). Basic extraction of the biogeographical signal as the inter-locality compositional similarity is often (if not automatically) done by classical hierarchical cluster analysis (hCA) and nonmetric multidimensional scaling (NMDS), applied to different specific time slices (sub-zones to stages). Both hCA and NMDS analyses are based on the preliminary computation of a symmetrical matrix of dissimilarity using a coefficient chosen a priori by the author (e.g. for taxonomic occurrence data, the Dice [= Sørensen = Bray–Curtis for presence/absence data], Simpson, or Jaccard coefficients; Shi 1993; Legendre and Legendre 2012). On the one hand, hCA focuses on the nested taxonomic relationships between assemblages and is therefore not suited for the identification of a gradational signal. On the other hand, NMDS (usually preferred to more conventional ordination techniques such as Principal Component Analysis or Principal Coordinates Analysis due to the non-Euclidean, semi-metric nature of the taxonomical space defined by most of these [dis]similarity coefficients) is intended to extract inter-gradational information in a low-dimensional reduced space and is therefore not well suited to the identification of hierarchical structures. As these two approaches are based on distinct assumptions about the nature of the inter-assemblage similarities embedded in the analyzed dataset, a comparison and combination of their results reinforces the confidence in the identified biogeographical structures. Nevertheless, although intuitive and widespread in our community, both methods also have several disadvantages (Brayard et al. 2007b). For instance, NMDS may misrepresent a gradational similarity structure in a 2D or 3D reduced space whereas analyzed objects are distinct in higher (unseen) dimensions of the reduced space. hCA and NMDS analyses for the Middle and Late Triassic time intervals are herein presented and discussed for the first time (Figs. 7.2 and

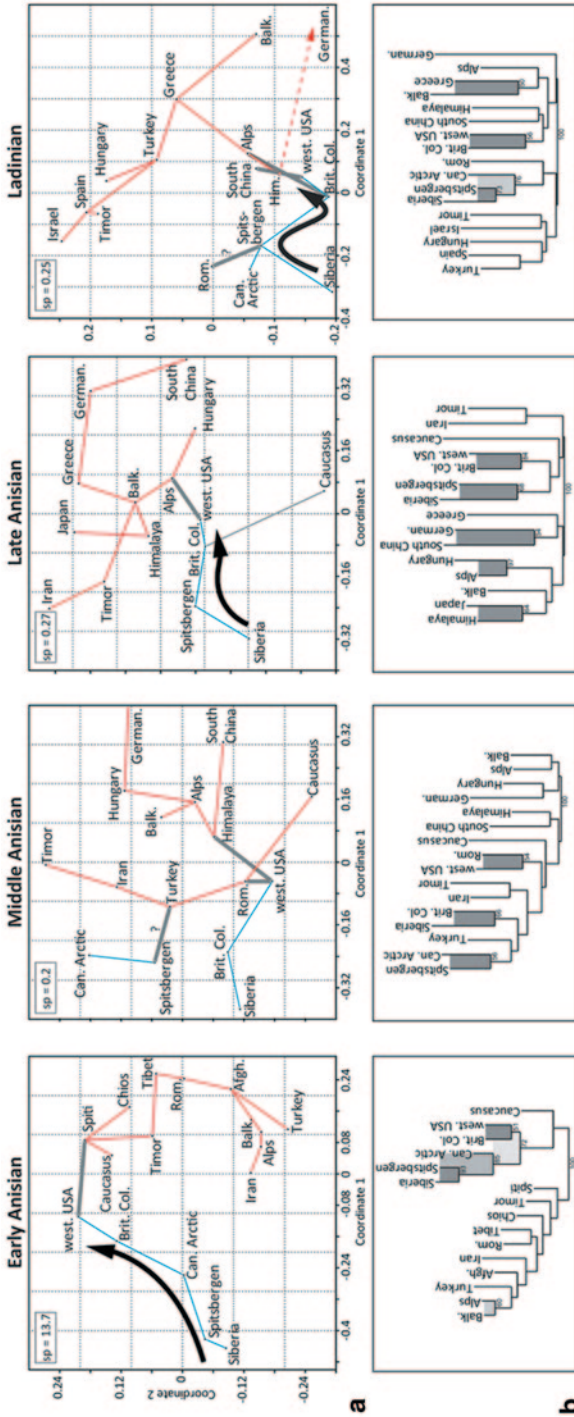


**Fig. 7.2** Biogeographical structuring for each stage of the Middle Triassic based on Bray–Curtis dissimilarity matrices (see Brayard et al. 2007b, 2009c for the Early Triassic). **a** Nonmetric Multidimensional Scaling map and superimposed Minimum Spanning Tree (stress is indicated by the Shepard plot [sp] value). *Black arrows* indicate gradational biogeographic structures. *Can.* Arctic Canadian Arctic, *Brit. Col.* British Columbia, *west. USA* western USA, *Balk.* Balkans, *Rom.* Romania, *German.* Germanic Basin, *Afgh.* Afghanistan. **b** Hierarchical Cluster analyses (bootstrap supports estimated with 1000 iterations; <50% when not indicated)

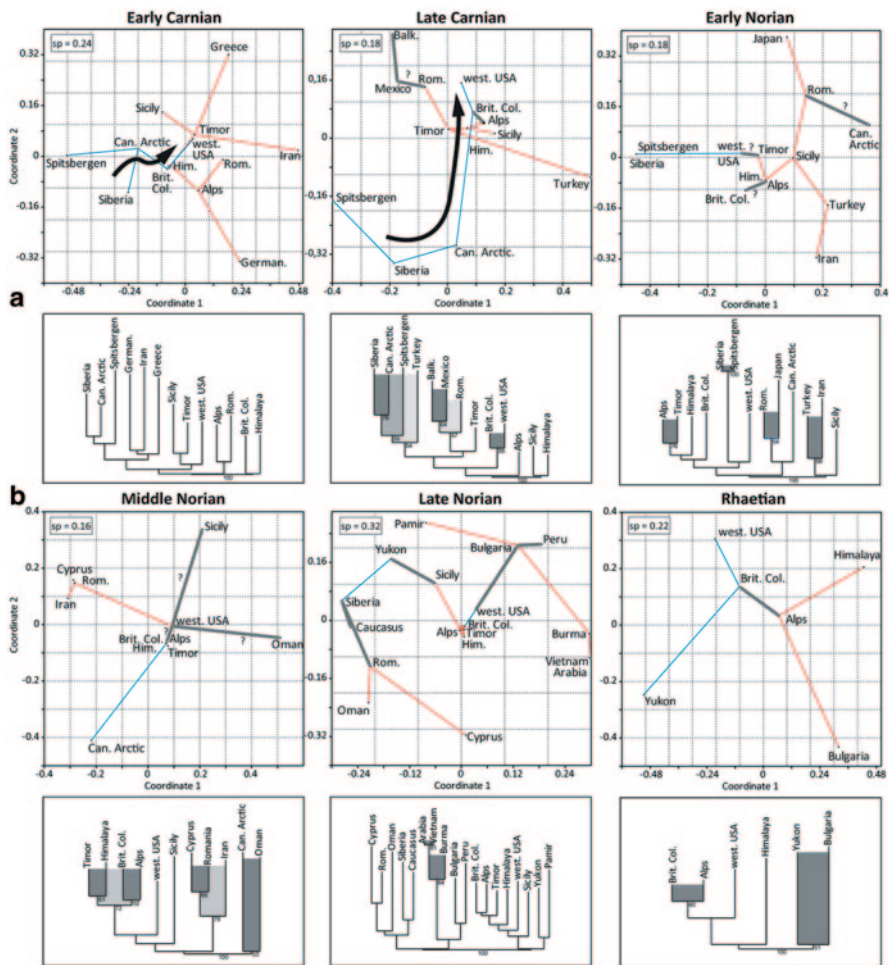


**Fig. 7.3** Biogeographical structuring for each stages of the Late Triassic based on Bray–Curtis dissimilarity matrices. (See Fig. 7.2 for details)

7.3; for computational details about these analyses and Early Triassic results, see Brayard et al. 2007b, 2009c).

Remarkably, hCA analyses rarely identify strongly supported biogeographical hierarchies for Middle and Late Triassic ammonoids. Only the early and late Anisian show clusters with support values greater than 50% and intuitive geographic associations. Complementary NMDS maps often better emphasize biogeographical differentiations especially between Tethyan and Panthalassic basins (early and late Anisian, Ladinian, Carnian, early Norian and Rhaetian), and a potential latitudinal structuring along the eastern Panthalassa (early and late Anisian, Ladinian, Carnian). Combining both methods, the middle Anisian, and the middle and late Norian do not show any well-defined biogeographical structuring.

## 7.2.2 *Recent Analytical Advances*

### 7.2.2.1 “Overall” Diversity Estimators

Based on the available (locality to basin-scale) occurrences of taxa among samples for each studied time bin, a bias-corrected incidence-based Chao’s estimator (Chao2; Chao 1984, 1987) and second-order jackknife estimator (Jackknife2; Smith and van Bell 1984) of “overall” (i.e. sampled + still unsampled) taxonomic richness can be computed. Both indices are well-known to ecologists (e.g. Walther and Moore 2005; Gotelli and Colwell 2011); they usually provide broadly similar results and are among the most reliable incidence-based nonparametric estimators of “overall” richness in ecological assemblages (Walther and Moore 2005). Nevertheless, in the context of paleobiogeographical studies, and according to the very nature of available data (often generic occurrences within basins), these quantities might not be viewed as statistical estimators of “overall” richness, but rather as indicators of (i) the sampling quality of the available fossil record and (ii) comparability of the inter-basinal structure of sampled incidence between the analyzed time bins (Brayard et al. 2009a; Escarguel ongoing work). Revised Chao2 estimates for the Early Triassic are given in Fig. 7.1, updating Brayard et al.’s (2009a) results.

### 7.2.2.2 Rarefaction and Extrapolation Curves

It is well known that the sampled taxonomic richness of a locality directly depends on the underlying sampling effort, and thus the available sample size. To circumvent this potential bias when comparing unevenly-sampled assemblages, ecologists and paleontologists traditionally use rarefaction methods as a means to “reduce” larger samples to the size of the smallest one, and then directly compare these rarefied richness estimates (Gotelli and Colwell 2001, 2011). However, this approach is not flawless. For instance, since the sample richness of a Tropical assemblage is usually far from its true richness due to the presence of many rare taxa, this can lead to a strongly underestimated rarefied richness when compared to the sample richness of a Boreal assemblage (Chao and Jost 2012). An alternate approach was recently offered by Chao and Jost (2012), who provided an elegant analytical solution for coverage-based rarefaction, “coverage” being a measure of sample completeness. Contrary to classical, sample size-based rarefaction, coverage-based rarefaction preserves the real degree of difference between the communities’ richnesses, even for small sample size, and provides a sampling “stopping rule”. Chao and Jost (2012) and Colwell et al. (2012) also provided an analytical solution for the extrapolation of sample richness to higher coverage instead of larger sample size, thus unifying coverage-based interpolation (rarefaction) and extrapolation into a single curve. Unified rarefaction and extrapolation curves for the 14 Triassic time intervals are given in Fig. 7.4.

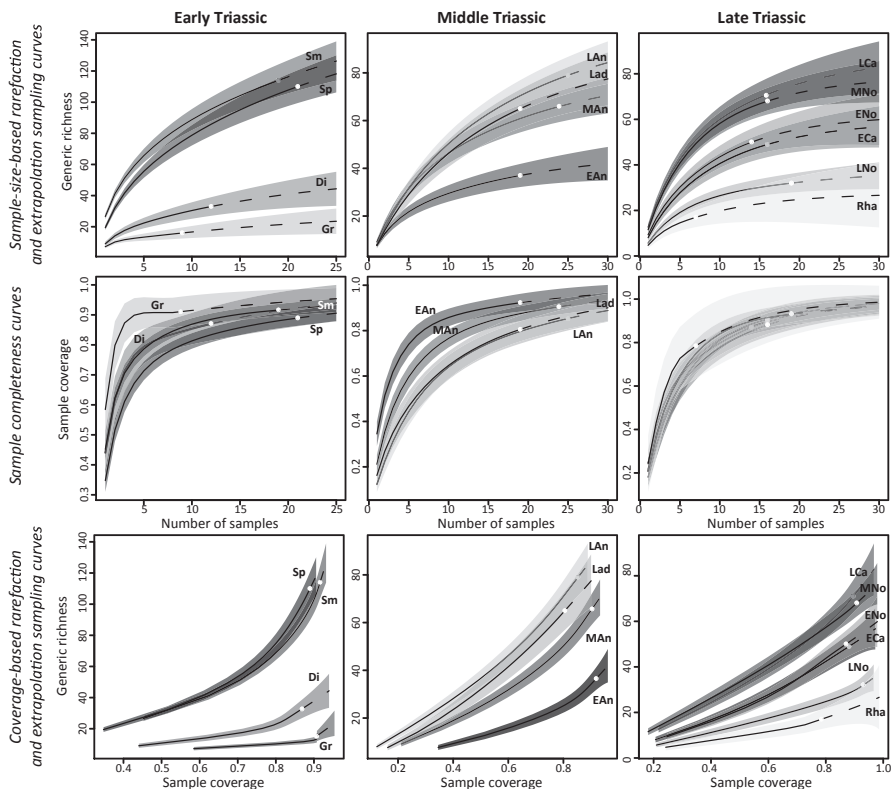


**Fig. 7.4** Rarefaction and extrapolation curves for the Triassic. *Solid lines*: interpolation curves; *dashed lines*: extrapolation curves; *white circles*: sample coverages. *Gr* Griesbachien, *Di* Dienerian, *Sm* Smithian, *Sp* Spathian, *EAn* early Anisian, *MAn* middle Anisian, *LAn* late Anisian, *Lad* Ladinian, *ECa* early Carnian, *LCa* late Carnian, *ENo* early Norian, *MNo* middle Norian, *LNo* late Norian, *Rha* Rhaetian

Sample-size rarefaction and extrapolation curves for the Early Triassic indicate that the estimated richness for the Smithian and Spathian is much higher than for the Griesbachian and Dienerian. However, all time intervals have rather similar sample coverage values (between  $\sim 0.85$  and  $\sim 0.92$ ), indicating that: (i) data can be directly compared to each other and are not likely to result from major sampling artifacts, and (ii) extrapolation is thus not needed. Sample coverages for the Dienerian and the Spathian being slightly lower than the two others, also suggest that the sampling effort for these two sub-stages is currently lower than for the Smithian and possibly also for the Griesbachian. Lower values of sample coverages for the late Anisian and Ladinian also point to the same hypothesis. Extrapolation may be useful in these two cases, suggesting higher estimated richnesses than for the early and late Anisian. Concerning the Late Triassic, only the Rhaetian value of sample coverage is lower than for other time intervals, which therefore can be directly compared to each other. Extrapolation curves for the Middle and Late Triassic intervals do not significantly change interpretations based on rarefaction.



### 7.2.2.3 Endemicity

The degree of endemicity (or, conversely, cosmopolitanism), i.e. the relative number of sampling units within which a given taxon occurs (hereafter called its “occurrence ratio”), is a fundamental life history trait directly or indirectly related to several other ecological and evolutionary features, from demographic dynamics to extinction probability (Gaston 1994; Kunin and Gaston 1997). Brayard et al. (2006) proposed an original approach to test the “occurrence ratio profile” (ORP) of a set of taxa against the null hypothesis of a random distribution of those taxa within the sampled localities. An ORP is a 10-bin histogram summarizing the frequency distribution of the occurrence ratio estimated for each sampled taxon. Confidence intervals are estimated for each ORP-bin through nonparametric bootstrap (random re-sampling of taxa with replacement), whereas a null ORP-model is generated by random permutation of taxa within localities, corresponding to the null hypothesis that, contrary to taxonomical richness (which remains unchanged by this permutation procedure), the taxonomical composition of each assemblage is not controlled by its geographic location and/or its environmental properties (permutation model #3 in Legendre et al. 1997). The ORPs and associated null-models for the 10 Middle and Late Triassic time intervals are given in Fig. 7.5 (see Brayard et al. 2006 for the Early Triassic ORPs).

While the early Anisian, Ladinian and late Norian empirical ORPs clearly match their associated null-distribution model, thus suggesting lack of strong geographical and/or environmental constraints in the distribution of taxa among the sampled basins, all other ORPs depart from this null model by showing: (i) more than expected highly endemic (o.r. < 0.1) and weakly to highly cosmopolitan (o.r. > 0.5) taxa, (ii) less than expected moderately endemic taxa ( $0.1 < \text{o.r.} < 0.2$ ), but (iii) frequencies of weakly endemic taxa ( $0.2 < \text{o.r.} < 0.5$ ) close to expectation from the null model. Lastly, the Rhaetian ORP suggests a contrasted situation with abundant highly endemic and moderately to highly cosmopolitan taxa, but without any weakly endemic to cosmopolitan genera. Nevertheless, this ultimate ORP must be interpreted cautiously, as it is based on a very small dataset, thus precluding any firm conclusion.

### 7.2.2.4 Biogeographic Relationships: A Network-Based Approach

The combined analysis of inter-assemblage taxonomical similarities through hierarchical clustering and ordination techniques is not flawless with respect to taxonomical occurrence or abundance data (Legendre and Legendre 2012). Critically, these techniques implicitly assume that such datasets define continuous and homogeneous topological spaces, which is generally not the case. As several combinations of taxa are a priori impossible for historical (phylogenetic and/or biogeographic) as well as functional (ecological) reasons, taxonomical data indeed define pretopological spaces where the concepts of similarity and neighborhood are formally decoupled (Čech 1966). In order to account for this major methodological constraint, Brayard et al. (2007b) developed an original approach leading to the visualization of a simi-

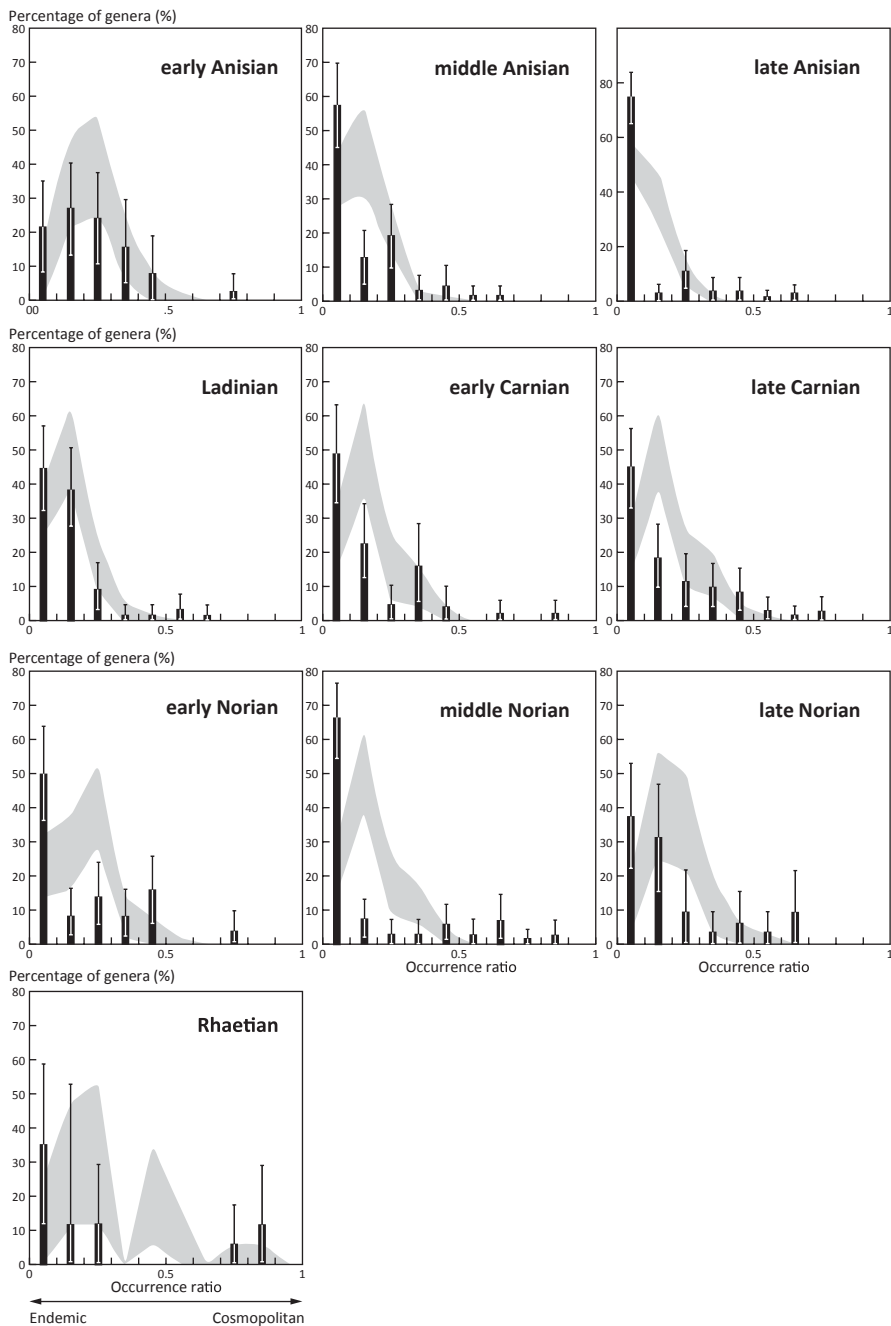


**Fig. 7.5** Generic Occurrence Ratio Profiles for Middle and Late Triassic ammonoids (see Brayard et al. 2006 for the Early Triassic). Bootstrapped 95% Confidence Intervals associated with the observed Occurrence Ratios (error bars on the histogram) estimated with 10,000 iterations; 95% ORP null distribution (*shaded area*) estimated with 10,000 iterations under a lottery permutation model (see Brayard et al. 2006 for details)

larity structure as a connected network of neighborhoods called a “bootstrapped spanning network” (BSN). Departing from a combined set of undirected “minimum spanning networks” (Prim 1957; Excoffier and Smouse 1994) nonparametrically bootstrapped from the sampled data, a BSN is computed by iterative removal, from the weakest links (i.e. links with lowest bootstrap supports) up to the best-supported ones, until: (i) the resulting network is no longer connected, or (ii) the overall product of bootstrap supports of the remaining links no longer increases (see Brayard et al. 2007b for algorithmic details). As a consequence, a BSN is not a “minimal” structure (the length of a link is not considered in the removing procedure), but rather “the simplest connected network best supported by the available data” (Brayard et al. 2007b, p. 755). Here, we illustrate the spatialized BSN corresponding to the 10 Middle and Late Triassic time intervals (Figs. 7.6, 7.7 and 7.8; see Brayard et al. 2007b, 2009c for the Early Triassic BSNs).

As expected, the BSNs demonstrate the latitudinal structuring of ammonoids in eastern Panthalassa as previously suggested by NMDS for the early and late Anisian and Ladinian (Fig. 7.2), but they also identify such a connection for the middle Anisian (Fig. 7.6). They modulate the Ladinian (Fig. 7.6) and Carnian (Fig. 7.7) latitudinal structuring in eastern Panthalassa as suggested by NMDS (Figs. 7.2 and 7.3), thus highlighting that links between localities are sometimes weak (Ladinian) or reticulate (Carnian). Moreover, the BSN provides additional precision about the other remaining Tethyan localities. For instance, dense connections in the western Tethys for the early Anisian are evidenced as well as the relative (middle to late Anisian) to near complete (Ladinian) isolation of the Germanic basin. The BSN also shows intertropical trans-Panthalassic connections during the Middle Triassic (Fig. 7.6). These links increase in number and change in latitude during the late Carnian (Fig. 7.7) and middle and late Norian (Fig. 7.8), suggesting a more cosmopolitan distribution of ammonoids at that time.

Visual investigation of the BSNs coupled with the paleogeographic location of the compared assemblages usually allows the identification of groups of related basins (here, two or three, depending on the time interval) whose differences in taxonomical composition can be further tested for significance against the null hypothesis of among-group random compositional differences. This can be done readily through one-way analysis of similarity (ANOSIM; Clarke 1993) or non-parametric multivariate analysis of variance (NP-MANOVA; Anderson 2001), in both cases using the same coefficient of taxonomical similarity (in this work, using the Dice [= Sørensen = Bray–Curtis for presence/absence data] coefficient). Although the ANOSIM procedure always appears more conservative (larger  $p$ -values) than NP-MANOVA, both techniques identify the very same time intervals as having significant differences among groups of taxonomical assemblages (Table 7.1). Whereas all Smithian to Ladinian time intervals return significant results indicating marked compositional differences between the Panthalassic and Tethyan realms, all Late Triassic time intervals but the 2-group early Norian test return non-significant results, suggesting a more homogeneous distribution of ammonoid genera between the two realms at that time. The two first Early Triassic time intervals show marginally-significant (Griesbachian) to non-significant (Dienerian) differences at a 5%-significance level, in both cases based on a small sample size, suggesting

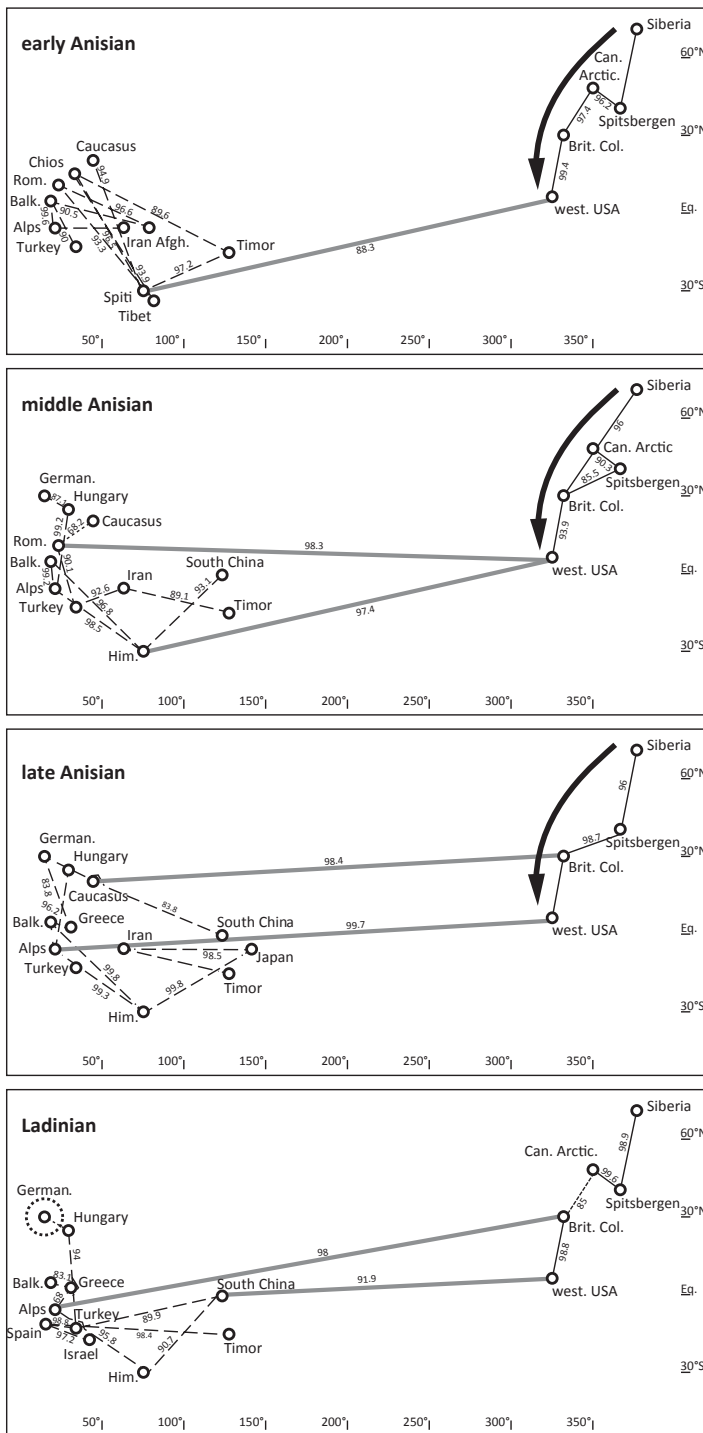


Fig. 7.6 Bootstrapped Spanning Networks for Middle Triassic ammonoids. Numbers indicate the bootstrap support values for each edge (100% when not reported; see Brayard et al. 2007b, 2009c

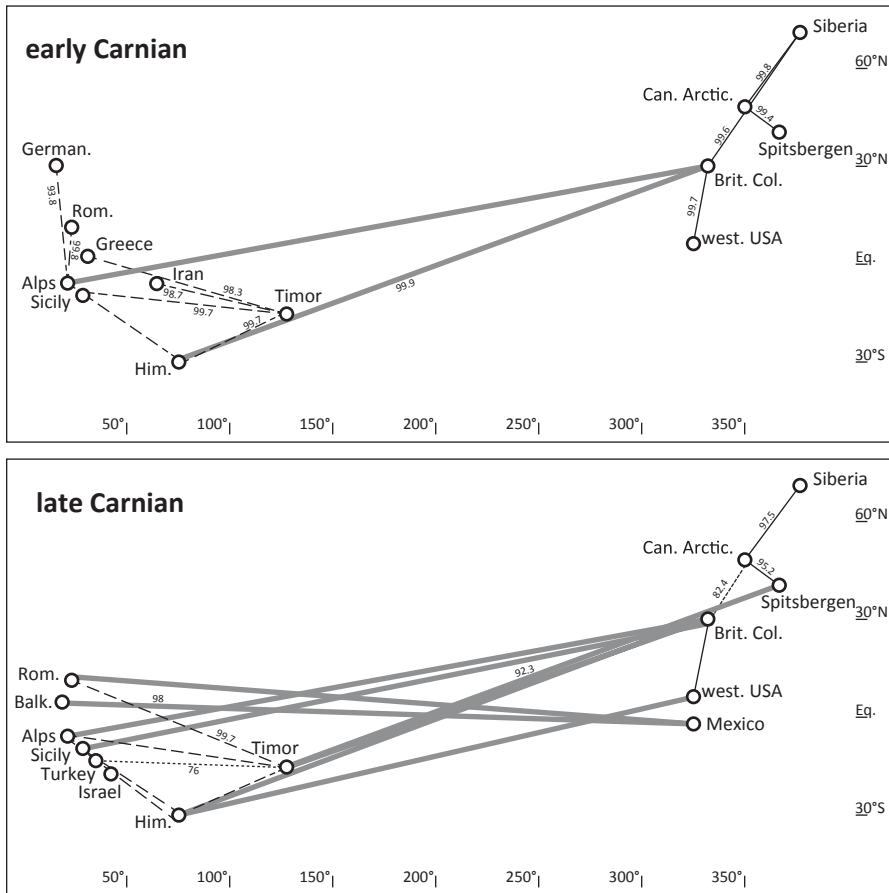


Fig. 7.7 Bootstrapped Spanning Networks for Carnian ammonoids. (See Fig. 7.6 for details)

the extremely low statistical power of such results, and thus lack of actual geographical structuring in these two cases. The early Anisian and Ladinian time intervals show a noteworthy configuration, as their respective ORPs do not depart from the null hypothesis of a random distribution of taxa within the sampled localities (see previous paragraph), whereas the present results demonstrate significant among-group compositional differences. These seemingly contradictory results point to taxonomically homogeneous groups of assemblages—hence a significant

---

for details and Early Triassic BSN). Paleolatitudes are approximated from Early Triassic maps (see Brayard et al. 2006) and arbitrarily considered to not vary too much between the Middle and Late Triassic for graphic convenience. *Black arrows* indicate observed latitudinal gradational biogeographic structures. *Bold dotted line* around the Germanic basin during the Ladinian illustrates the isolation of this basin at that time.

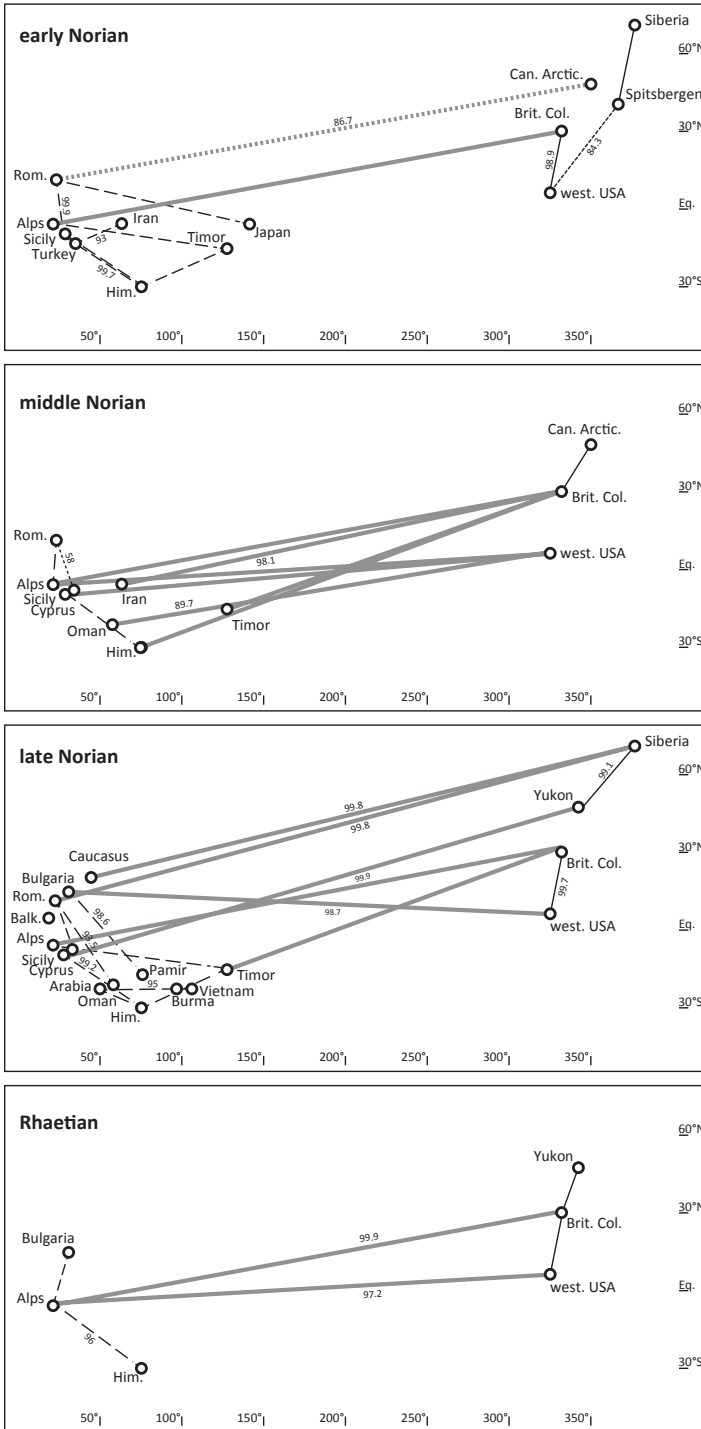


Fig. 7.8 Bootstrapped Spanning Networks for Norian and Rhaetian ammonoids. (See Fig. 7.6 for details)

**Table 7.1** One-way ANOSIM and NP-MANOVA results, showing the Triassic time intervals with significantly different groups of taxonomical assemblages. Two-group partitioning: Eastern Panthalassa vs. Tethys; three-group partitioning: Eastern Panthalassa vs. Eastern Tethys vs. Western Tethys. Contrast analysis: ANOSIM- or NP-MANOVA-based pairwise comparisons, including a sequential Bonferroni correction for multiple testing

	ANOSIM		NP-MANOVA		Contrast analysis (pairwise comparisons, identifying groups of assemblages with significant differences)
	R	P	pseudo-F	p	
Griesbachian (2 gr.)	0.307	0.0285*	3.33	0.0285*	East. Panthalassa-Tethys
Dienerian (2 gr.)	0.207	0.054 NS	2.77	0.062 NS	None
Smithian (2 gr.)	0.246	0.006**	3.63	0.0032**	East. Panthalassa-Tethys
Spathian (3 gr.)	0.317	0.0025**	3.34	0.0008***	All (NP-MANOVA); all but West.-East. Tethys (ANOSIM)
Early Anisian (2 gr.)	0.841	0.0002***	11.09	0.0002***	East. Panthalassa-Tethys
Early Anisian (3 gr.)	0.553	0.00024***	6.33	0.00013***	East. Panthalassa-West. and East. Tethys
Middle Anisian (3 gr.)	0.295	0.01*	2.36	0.0056**	East. Panthalassa-West. Tethys
Late Anisian (3 gr.)	0.326	0.0023**	2.31	0.0002***	All (NP-MANOVA); all but West.-East. Tethys (ANOSIM)
Ladinian (3 gr.)	0.489	0.00006***	2.72	0.0001***	All
Early Carnian (3 gr.)	0.127	0.123 NS	1.445	0.075 NS	None
Late Carnian (3 gr.)	0.037	0.35 NS	1.21	0.24 NS	None
Early Norian (2 gr.)	0.375	0.01*	2.54	0.0045**	East. Panthalassa-Tethys
Early Norian (3 gr.)	0.096	0.21 NS	1.44	0.13 NS	None
Middle Norian (2 gr.)	-0.017	0.47 NS	0.813	0.61 NS	None
Middle Norian (3 gr.)	-0.028	0.58 NS	0.872	0.64 NS	None
Late Norian (3 gr.)	0.080	0.17 NS	1.352	0.165 NS	None
Rhaetian (2 gr.)	0.352	0.10 NS	1.69	0.20 NS	None

NS  $p \geq 0.05$ ; \* $p \geq 0.01$ ; \*\* $p \geq 0.001$ ; \*\*\* $p < 0.001$

biogeographical structuring—where taxa tend to be relatively widespread within their group—hence a lack of highly-endemic genera.

Lastly, when a non-random compositional difference is detected by the ANOSIM and NP-MANOVA procedures, a SIMPER analysis (Clarke 1993) allows the identification of those taxa most contributing to the among-group “overall average dissimilarity” (OAD, using the same coefficient of taxonomic similarity as used

**Table 7.2** SIMPER results for Triassic time intervals showing ANOSIM- and NP-MANOVA-based significant differences among groups of taxonomic assemblages (same group-partitioning as in Table 7.1). OAD: among-group overall average dissimilarity;  $N_{50\%}$ ,  $N_{80\%}$ : number (percentage) of genera contributing to 50% and 80% of OAD, respectively; List of the  $N_{50\%}$  genera: genera contributing to 50% of OAD, ranked in order of decreasing contribution to OAD

Time interval	OAD	$N_{50\%}$ , $N_{80\%}$	List of the $N_{50\%}$ genera
Smithian (2 gr.)	55.6	19 (31%), 34 (56%)	<i>Melagathiceras</i> , <i>Clypeoceras</i> , <i>Prionolobus</i> , <i>Anaxenaspis</i> , <i>Arctoceras</i> , <i>Pseudoceltites</i> , <i>Euflemingites</i> , <i>Paranannites</i> , <i>Aspenites</i> , <i>Inyoites</i> , <i>Owenites</i> , <i>Flemingites</i> , <i>Wyomingites</i> , <i>Cordillerites</i> , <i>Prionites</i> , <i>Juvenites</i> , <i>Wasachites</i> , <i>Xenoceltites</i> , <i>Kashmirites</i>
Spathian (3 gr.)	70.8	24 (26%), 49 (53%)	<i>Procladiscites</i> , <i>Keyserlingites</i> , <i>Sulioticeras</i> , <i>Prohungarites</i> , <i>Cordillerites</i> , <i>Columbites</i> , <i>Isculitoides</i> , <i>Stacheites</i> , <i>Metadagnoceras</i> , <i>Subcolumbites</i> , <i>Tirolites</i> , <i>Zenoites</i> , <i>Albanites</i> , <i>Procarmites</i> , <i>Ussurites</i> , <i>Proptychitoides</i> , <i>Leiophyllites</i> , <i>Paragoceras</i> , <i>Nordophiceras</i> , <i>Fengshanites</i> , <i>Dagnoceras</i> , <i>Dalmatites</i> , <i>Hemilecanites</i> , <i>Pseudodinarites</i>
Early Anisian (2 gr.)	80.3	10 (27%), 21 (57%)	<i>Lenotropites</i> , <i>Ussurites</i> , <i>Discogymnites</i> , <i>Grambergia</i> , <i>Stenopopanoceras</i> , <i>Gymnites</i> , <i>Psilosturia</i> , <i>Karangatites</i> , <i>Leiophyllites</i> , <i>Sturia</i>
Early Anisian (3 gr.)	69.9	10 (27%), 20 (54%)	<i>Psilosturia</i> , <i>Ussurites</i> , <i>Grambergia</i> , <i>Sturia</i> , <i>Lenotropites</i> , <i>Stenopopanoceras</i> , <i>Aegeiceras</i> , <i>Discogymnites</i> , <i>Paracrochordiceras</i> , <i>Gymnites</i>
Middle Anisian (3 gr.)	77.8	18 (27%), 36 (55%)	<i>Ussurites</i> , <i>Anagymnotoceras</i> , <i>Acrochordiceras</i> , <i>Balatonites</i> , <i>Gymnites</i> , <i>Intornites</i> , <i>Norites</i> , <i>Proarcestes</i> , <i>Megaphyllites</i> , <i>Stenopopanoceras</i> , <i>Ptychites</i> , <i>Bulogites</i> , <i>Ismidites</i> , <i>Proteusites</i> , <i>Nicomedites</i> , <i>Sageceras</i> , <i>Discoptychites</i> , <i>Beyrichites</i>
Late Anisian (3 gr.)	89.0	17 (21.5%), 39 (49%)	<i>Gymnites</i> , <i>Frechites</i> , <i>Nevadites</i> , <i>Intornites</i> , <i>Japonites</i> , <i>Proarcestes</i> , <i>Monophyllites</i> , <i>Kellnerites</i> , <i>Flexoptychites</i> , <i>Longobardites</i> , <i>Judicarites</i> , ? <i>Megaphyllites</i> , <i>Paraceratites</i> , <i>Amphipopanoceras</i> , <i>Epigymnites</i> , <i>Reitziites</i> , <i>Parapopanoceras</i>
Ladinian (3 gr.)	84.7	15 (23%), 33 (51%)	<i>Istreites</i> , <i>Proarcestes</i> , <i>Indigirites</i> , <i>Asklepioceras</i> , <i>Protrachyceras</i> , <i>Argolites</i> , <i>Sphaerocladiscites</i> , <i>Daxatina</i> , <i>Frankites</i> , <i>Muensterites</i> , <i>Arpadites</i> , <i>Arctoptychites</i> , <i>Longobardites</i> , <i>Thanamites</i> , <i>Iberites</i>
Early Norian (2 gr.)	84.5	9 (18%), 23 (47%)	<i>Hypocladiscites</i> , <i>Paracladiscites</i> , <i>Pterosirenites</i> , <i>Cladiscites</i> , <i>Dimorphites</i> , <i>Juvavites</i> , <i>Arcestes</i> , <i>Griesbachites</i> , <i>Thisbites</i>

by the ANOSIM and NP-MANOVA), based on an additive decomposition of the contribution of each taxon to OAD (Table 7.2). In all cases studied here, ~25 % of the genera together generate half of the overall average compositional dissimilarity



among groups of basins (~50% controlling 80% of OAD), highlighting the uneven contribution of each genus to the overall biogeographic signal. It is worth noting here that the lists of those genera driving the biogeographic differentiation bring together long- and short-ranging taxa, suggesting that ammonoid longevity is not strongly related to their endemism level, a rather counterintuitive result that remains to be further investigated.

## 7.3 Exploring Revised Data: Refining Patterns and Underlying Processes

### 7.3.1 *Early Triassic*

Updated generic richness (GR) patterns for the Early Triassic are given in Fig. 7.1. Compared to Brayard et al. (2009a), the rapid rediversification of ammonoids is still obvious, with even higher estimated total GR for the Griesbachian, Dienerian and Smithian, which is a direct consequence of the numerous detailed monographs published recently from various areas (Shigeta and Zakharov 2009; Jenks et al. 2010; Ware et al. 2011; Brühwiler et al. 2012a, 2012b, 2012c; Zakharov and Mousavi Abnavi 2013). Unpublished Spathian data still lead to the underestimation of its GR, which is likely above the Smithian value. Evolution of the Early Triassic GR was already detailed in Brayard et al. (2009a).

The existence of a latitudinal gradient of generic richness (LGGR) was the first Early Triassic large-scale biogeographical pattern investigated based on a taxonomically homogeneous dataset (Brayard et al. 2006, 2007b). Based on a basin-level spatial resolution allowing realistic reconstruction of large-scale biogeographical patterns, this analysis departed from previously published macroecological studies on past diversity patterns. The results of this work mainly indicated that the global first-order trend in increasing ammonoid diversity was accompanied by a progressive change from cosmopolitan to latitudinally-restricted distribution during the Early Triassic (Brayard et al. 2006). This led to the emergence of a clear latitudinal diversity gradient during most of the Smithian and Spathian sub-stages (Brayard et al. 2006, Fig. 11). Based on the likely assumption that ammonoids were temperature-sensitive organisms, this also strongly suggests the progressive appearance of a marked latitudinal temperature gradient during the Early Triassic, with maximum differentiation during the Smithian and Spathian (see also Kummel 1973b and Dagens 1988, 1997). However, this global trend was not a continuous process as it was interrupted at least once during a brief episode of ammonoid cosmopolitanism combined with a marked extinction event during the end-Smithian (e.g. Tozer 1981b, 1982; Dagens 1988, Brayard et al. 2006).

Brayard et al. (2006) also used quantitative analyses of endemism based on the ORP to complete their study on the biogeographical structuring of faunas. They clearly indicated a rapid increase in the percentage of endemic genera concomitant

with the edification of the LGGR, notwithstanding a sudden return to a cosmopolitan structuring during the end-Smithian (Brayard et al. 2006, Figs. 7–9).

The biogeographical structure of faunal assemblages was also explored by means of coupled hCA, NMDS and BSN analyses (Brayard et al. 2007b, 2009c). These three combined approaches provided further evidences for an increase in steepness of the latitudinal temperature gradient during the Early Triassic. In particular, identified inter-locality relationships confirmed that the very beginning of the Early Triassic (Griesbachian) corresponds to a very simple biogeographical setting with assemblages dominated by common cosmopolitan genera. This context shifts rapidly to a more heterogeneous configuration (as confirmed here by the NP-MANOVA and ANOSIM comparisons of Tethyan vs. Panthalassic assemblages; Tables 7.1 and 7.2), indicative of a more endemic and latitudinally-restricted distribution of ammonoids during the Smithian and Spathian. Nevertheless, BSN results also highlight the development of a marked intertropical faunal belt across the Tethys and Panthalassa at that time, due to the co-occurrence of certain ammonoid genera on opposite sides of the Panthalassa illustrating latitudinally-restricted faunal exchanges during the Smithian (Brayard et al. 2009b, 2013; Jenks et al. 2010), Spathian (Galfetti et al. 2007a; Guex et al. 2010) and end-Spathian (Monnet et al. 2013).

The formation of an ammonoid LGGR during the Early Triassic is likely concomitant with the emergence of a latitudinal temperature gradient in the world ocean. The end-Smithian event has been qualitatively recognized for over 30 years (Tozer 1982; Dagys 1988), but its potential causes remained elusive until recently. Indeed, the rapid collapse of the ammonoid LGGR, the common occurrence of low diversity and cosmopolitan faunas and the high taxonomic similarities among regional assemblages clearly point to a global oceanographic and climatic event such as a return to a weak latitudinal temperature gradient (Brayard et al. 2006, 2007b, 2009c). Additional evidence of a global end-Smithian event first came from various palynological, sedimentological and geochemical analyses (Galfetti et al. 2007a, 2007b, 2007c). Recent  $\delta^{18}\text{O}$  isotopic analyses measured on conodont apatite, provide a good proxy for sea-surface temperatures and indicate that the Smithian-Spathian boundary was accompanied by a  $\sim 8^\circ\text{C}$  drop down in the Tethys (Romano et al. 2013).

Most if not all Early Triassic ammonoids are very likely derived from a single PT-survivor species. They thus represent an ideal case of a “quasi-monophyletic” clade evolving in a stable geologic framework, only depending on the oceanographic setting (SST, currents, etc.), Brayard et al. (2004) ran their “geophyletic model” (Brayard et al. 2004, 2005; Escarguel et al. 2008) using Early Triassic paleogeography to simulate the Early Triassic diversification and diversity distribution of ammonoids. The “geophyletic model” is a serial automaton simulation model of the “General Simulation Model” family (Gotelli et al. 2009); it has been shown to produce realistic large-scale diversity patterns under extant geographic and oceanographic settings (Brayard et al. 2005; Escarguel et al. 2008). The principal result of these simulations is that the formation of a LGGR basically depends on the shape and magnitude of the SST gradient, corroborating the working hypothesis of a direct causal link between changes in the SST gradient and the LGGR.

### 7.3.2 *Middle Triassic*

Ammonoid-based quantitative and global-scale analyses for Middle Triassic time intervals are much scarcer in the literature than for the Early Triassic, in that most of the known biogeographical patterns are only qualitatively characterized (Fig. 7.1). The Spathian/Anisian boundary is characterized by a marked faunal turnover associated with the radiation of mid-Triassic families such as Arcestidae (Dagys et al. 1979; Monnet and Bucher 2005; Konstantinov 2008; Balini et al. 2010). During the Anisian, latitudinal differentiation of assemblages seems to be maintained at levels comparable to the Smithian or Spathian (Galfetti et al. 2007c; Balini et al. 2010), which suggests a lingering tight link between the SST gradient and the LGGR. As shown here, the BSN approach underlines a clear latitudinalisation of the biogeographical structures with a northeastern Panthalassic gradient during the Middle Triassic (Fig. 7.6). Faunal heterogeneity also seems to have increased globally from the early Anisian to the late Anisian, as suggested by the increasing among-group overall average dissimilarity (OAD; Table 7.2), possibly due to climatic fluctuations (Zakharov et al. 2008) or tectono-eustatic events such as transgression on various epicontinental seas (Balini et al. 2010). For instance, beginning in the late Anisian, a significant number of endemic taxa repeatedly developed within the Germanic basins, where the endemism level fluctuated according to successive immigration events enabled by transgressions and corridors openings (Urlichs and Mundlos 1985; Klug et al. 2005). This is well illustrated by BSN analyses (Fig. 7.6) where the Germanic basin appears to be almost completely isolated from other localities during the late Anisian and Ladinian. This led to transient regional diversity hotspots that oftentimes complicated large-scale accurate correlation (e.g. Monnet and Bucher 2005, 2006b). The middle/late Anisian transition and the late Anisian are marked by an increase in taxa shared by both sides of the Panthalassa, but particularly more so along the western coast of Pangea (Dagys 1988; Monnet and Bucher 2005; Monnet et al. 2007, 2008). This biogeographic structuring is well confirmed by BSN results (Fig. 7.6). In contrast with the Anisian, Ladinian ammonoids are customarily assumed to be more cosmopolitan with extremely similar assemblages across latitudes, Tethys and the Panthalassa (Tozer 1981b; Dagys 1988). However, we provide evidence here with BSN analyses (Fig. 7.6) that a biogeographical latitudinal structure of faunal relationships persists during the Ladinian along the eastern Panthalassa, although possibly somewhat weaker than during the Anisian (see also Konstantinov 2008). A marked differentiation between the Tethys and Panthalassic basins is also confirmed by the NP-MANOVA and ANOSIM comparisons (Table 7.1), again indicative of rather heterogeneous distributions of ammonoids during the Ladinian. Nevertheless, the related ORP (Fig. 7.5) does not indicate an excess of moderately to highly endemic genera (o.r. < 0.2), showing that such structuring is driven by genera that are relatively well distributed within their respective biogeographical realms.

### 7.3.3 Late Triassic

Previous works on the biogeographical structuring of the Late Triassic have been mostly qualitative. Successive episodes of extinction and radiation (e.g. at the base of the late Carnian) are well known from the Carnian and Norian. However, the biogeographical differentiation of ammonoid faunas is more or less identical during both intervals, with an apparent marked LGGR that is probably due mainly to the paucity of the Boreal record (Dagys 1988; Balini et al. 2010). Boreal assemblages also appear rather endemic, but cosmopolitan genera persist, facilitating large-scale correlation (Balini et al. 2010). While both early and late Carnian BSNs clearly indicate an eastern Panthalassa latitudinal structuring (see also Konstantinov and Sobolev 2004), the intensity of biogeographical relationships between the Tethyan and Panthalassic realms markedly increases through time (Fig. 7.7). A weak but significant biogeographical distinction reappears during the early Norian (Fig. 7.8), as also evidenced by the NP-MANOVA and ANOSIM analyses (Table 7.1). However, this pattern does not hold true with a closer time resolution because the earliest early Norian ammonoid faunas from British Columbia clearly show boreal influences (Balini et al. 2012b), while those of the late Early Norian are more similar to those from the Tethys. Middle and late Norian BSNs do not show any clear pattern, illustrating the return to a globally homogeneous biogeographical configuration.

The base of the late Norian is characterized by the appearance of the first heteromorphic genus (*Rhabdoceras*) and the Rhaetian by the numerical increase in heteromorph taxa. These heteromorphs appear rather common, but known Rhaetian occurrences still remain scarce (e.g. Dagys et al. 1979; Tozer 1994), thus preventing any firm biogeographical interpretation, as also shown by the BSN based on the entire fauna (Fig. 7.8).

## 7.4 What's on the Horizon?

Until now, macroevolution, biogeography and macroecology have remained relatively independent research fields. However, bringing them together in a unified, descriptive and predictive approach offers new exciting perspectives in the understanding of modern and past biodiversity drivers and dynamics (Escarguel et al. 2011). This fertile cross-field emulation addresses new questions, such as how -and to what extent- biogeographical and macroecological properties of taxa are influenced by their evolutionary history? Because the fragmentary nature of the fossil record makes abundance information unreliable in most cases, we only considered here the taxonomic richness aspect of biodiversity. Yet, the biodiversity concept involves other dimensions also robust to the fossilization process, such as phylogenetic diversity (e.g. Emerson and Gillespie 2008), ecological (functional) diversity (e.g. Petchey and Gaston 2006), or morphological disparity (e.g. Foote 1997; Villier and Korn 2004; McGowan 2005). Based on previously acquired data and results, the objectives of future studies will be therefore to quantitatively assess and compare

spatial and temporal dynamics of these complementary aspects of biodiversity, as well as their potential relationships with major biotic and abiotic parameters such as geographic rarity, taxon longevity, extinction probability, or climate.

From this point of view, the understanding of past biodiversity might be first investigated by exploring the intricate and multidimensional relationships among phylogenetic, geographic and morphological distances and their evolution through geological time since some of these properties are now available through large revised datasets (e.g., for Triassic ammonoids, Brayard et al. 2009a; Brayard and Escarguel 2013; Brosse et al. 2013). In the context of Triassic studies, such a multidimensional approach to biodiversity is expected to significantly improve our understanding of the Early Triassic biotic recovery (e.g. do latitudinal gradients in phylogenetic, functional or morphological diversity also emerge parallel to the LGGR?) as well as the Late Triassic long and rough road to the Triassic/Jurassic crisis (e.g. do the end Norian and Rhaetian extinction events show any structuring in phylogenetic, ecological or morphological loss?). In all cases, significant results and new questions are expected from integration of quantitative descriptions of diversity dynamics based on fossils already available as well as new fossils integrated in taxonomically-revised, geo-referenced datasets. When combined with more inductive, simulation-based approaches, this will allow the identification of the underlying evolutionary and functional processes, as well as the relative importance of potential parameters driving the observed patterns (see Brayard et al. 2004 for a preliminary example on Early Triassic ammonoid generic richness).

**Acknowledgments** We thank M. Balini and D. Korn for their constructive comments and suggestions. The CNRS INSU Intervie and the Région Bourgogne supported A.B. and G.E. for this study. This is also a contribution to the ANR project AFTER (ANR-13-JS06-0001). HB acknowledges the support of the Swiss National Science Foundation (project 200021\_135446).

## References

- Anderson MJ (2001) A new method for non-parametric multivariate analysis of variance. *Austral Ecol* 26:32–46
- Balini M, Lucas SG, Jenks JF, Spielmann JA (2010) Triassic ammonoid biostratigraphy: an overview. In: Lucas SG (ed) *The Triassic timescale*. The Geological Society of London, London
- Balini M, Jenks JF, Martin R (2012a) Taxonomy and stratigraphic significance of *Trachyceras silberlingi* n. sp., from the lower Carnian of South Canyon (New Pass Range, Central Nevada, USA). *Boll Soc Paleont Ital* 51:127–136
- Balini M, Krystyn L, Levera M, Tripodo A (2012b) Late Carnian-Early Norian ammonoids from the GSSP candidate section Pizzo Mondello (Sicani Moutains, Sicily). *Riv Ital Paleont Strat* 118:47–84
- Beaugrand G, Rombouts I, Kirby R (2013) Towards an understanding of the pattern of biodiversity in the oceans. *Global Ecol Biogeogr* 22:440–449
- Brayard A, Bucher H (2008) Smithian (early Triassic) ammonoid faunas from northwestern Guangxi (South China): taxonomy and biochronology. *Foss Strata* 55:1–179
- Brayard A, Bucher H (2015) Permian-Triassic extinctions and rediversifications. This volume
- Brayard A, Escarguel G (2013) Untangling phylogenetic, geometric and ornamental imprints on Early Triassic ammonoid biogeography: a similarity-distance decay study. *Lethaia* 46:19–33

- Brayard A, Hérán M-A, Costeur L, Escarguel G (2004) Triassic and Cenozoic palaeobiogeography: two case studies in quantitative modeling using IDL. *Palaeontol Electron* 7:22.
- Brayard A, Escarguel G, Bucher H (2005) Latitudinal gradient of taxonomic richness: combined outcome of temperature and geographic mid-domains effects? *J Zool Syst Evol Res* 43:178–188
- Brayard A, Bucher H, Escarguel G, Fluteau F, Bourquin S, Galfetti T (2006) The Early Triassic ammonoid recovery: paleoclimatic significance of diversity gradients. *Palaeogeogr Palaeoclim Palaeoecol* 239:374–395
- Brayard A, Bucher H, Brühwiler T, Galfetti T, Goudemand N, Guodun K, Escarguel G, Jenks J (2007a) *Proharpoceras* Chao: a new ammonoid lineage surviving the end-Permian mass extinction. *Lethaia* 40:175–181
- Brayard A, Escarguel G, Bucher H (2007b) The biogeography of Early Triassic ammonoid faunas: clusters, gradients and networks. *Geobios* 40:749–765
- Brayard A, Escarguel G, Bucher H, Monnet C, Brühwiler T, Goudemand N, Galfetti T, Guex J (2009a) Good genes and good luck: ammonoid diversity and the end-Permian mass extinction. *Science* 325:1118–1121
- Brayard A, Brühwiler T, Bucher H, Jenks J (2009b) *Guodunites*, a low-palaeolatitude and trans-Panthalassic Smithian (Early Triassic) ammonoid genus. *Palaeontology* 52:471–481
- Brayard A, Escarguel G, Bucher H, Brühwiler T (2009c) Smithian and Spathian (Early Triassic) ammonoid assemblages from terranes: paleoceanographic and paleogeographic implications. *J Asian Earth Sci* 36:420–433
- Brayard A, Bylund KG, Jenks JF, Stephen D, Olivier N, Escarguel G, Fara E, Vennin E (2013) Smithian ammonoid faunas from Utah: implications for Early Triassic biostratigraphy, correlation and basinal paleogeography. *Swiss J Palaeontol* 132:141–219
- Brosse M, Brayard A, Fara E, Neige P (2013) Ammonoid recovery after the Permian–Triassic mass extinction: a re-exploration of morphological and phylogenetic diversity patterns. *J Geol Soc (London)* 170:225–236
- Brühwiler T, Bucher H, Goudemand N, Galfetti T (2012a) Smithian (Early Triassic) ammonoid faunas from Exotic Blocks from Oman: taxonomy and biochronology. *Palaeontogr A* 296:3–107
- Brühwiler T, Bucher H, Krystyn L (2012b) Middle and late Smithian (Early Triassic) ammonoids from Spiti (India). *Spec Pap Palaeontol* 88:115–174
- Brühwiler T, Bucher H, Ware D, Hermann E, Hochuli PA, Roohi G, Rehman K, Yassen A (2012c) Smithian (Early Triassic) ammonoids from the Salt Range. *Spec Pap Palaeontol* 88:1–114
- Čech E (1966) *Topological spaces*. Wiley, London
- Chao A (1984) Nonparametric estimation of the number of classes in a population. *Scand J Stat* 11:265–270
- Chao A (1987) Estimating the population size for capture-recapture data with unequal catchability. *Biometrics* 43:783–791
- Chao A, Jost L (2012) Coverage-based rarefaction and extrapolation: standardizing samples by completeness rather than size. *Ecology* 93:2533–2547
- Clarke KR (1993) Non-parametric multivariate analyses of changes in community structure. *Aust J Ecol* 18:117–143
- Colwell RK, Rahbek C, Gotelli NJ (2005) The mid-domain effect: there's a baby in the bathwater. *Am Nat* 166:E149–E154
- Colwell RK, Chao A, Gotelli NJ, Lin S-Y, Mao CX, Chazdon RL, Longino JT (2012) Models and estimators linking individual-based and sample-based rarefaction, extrapolation and comparison of assemblages. *J Plant Ecol* 5:3–21
- Connolly SR, Bellwood DR, Hughes TP (2003) Indo-Pacific biodiversity of coral reefs: deviations from a mid-domain model. *Ecology* 84:2178–2190
- Dagys AS (1988) Major features of the geographic differentiation of Triassic ammonoids. In: Wiedmann J, Kullmann J (eds) *Cephalopods—present and past*. Schweizerbart, Stuttgart
- Dagys AS (1997) A new late Olenekian (Triassic) ammonoid of low paleolatitude affinity from Arctic Asia (Eastern Taimyr). *Paläontol Z* 71:217–220
- Dagys AS, Ermakova SV (1990) Early Olenekian ammonoids of Siberia. *Nauka, Moscow*
- Dagys AS, Arkhipov YV, Bychkov YM (1979) *Stratigraphy of the Triassic System of the North-eastern Asia*. Nauka, Moscow

- Dera G, Neige P, Dommergues J-L, Brayard A (2011) Ammonite paleobiogeography during the Pliensbachian–Toarcian crisis (Early Jurassic) reflecting paleoclimate, eustasy, and extinctions. *Global Planet Change* 78:92–105
- Dommergues J-L, Fara E, Meister C (2009) Ammonite diversity and its palaeobiogeographical structure during the early Pliensbachian (Jurassic) in the western Tethys and adjacent areas. *Palaeogeogr Palaeoclim Palaeoecol* 280:64–77
- Emerson BC, Gillespie RG (2008) Phylogenetic analysis of community assembly and structure over space and time. *Trends Ecol Evol* 23:19–630
- Escarguel G, Bucher H (2004) Counting taxonomic richness from discrete biochronozones of unknown duration: a simulation. *Palaeogeogr Palaeoclim Palaeoecol* 202:181–208
- Escarguel G, Brayard A, Bucher H (2008) Evolutionary rates do not drive latitudinal diversity gradients. *J Zool Syst Evol Res* 46:82–86
- Escarguel G, Fara E, Brayard A, Legendre S (2011) Biodiversity is not (and never has been) a bed of roses! *C R Biol* 334:351–359
- Excoffier L, Smouse PE (1994) Using allele frequencies and geographic subdivision to reconstruct gene trees within a species: molecular variance parsimony. *Genetics* 136:343–359
- Foote M (1992) Rarefaction analysis of morphological and taxonomic diversity. *Paleobiology* 18:1–16
- Foote M (1997) The evolution of morphological diversity. *Annu Rev Ecol Syst* 28:129–152.
- Galfetti T, Bucher H, Ovtcharova M, Schaltegger U, Brayard A, Brühwiler T, Goudemand N, Weissert H, Hochuli PA, Cordey F, Guodun KA (2007a) Timing of the Early Triassic carbon cycle perturbations inferred from new U-Pb ages and ammonoid biochronozones. *Earth Planet Sci Lett* 258:593–604
- Galfetti T, Bucher H, Brayard A, Hochuli PA, Weissert H, Guodun K, Atudorei V, Guex J (2007b) Late Early Triassic climate change: insights from carbonate carbon isotopes, sedimentary evolution and ammonoid paleobiogeography. *Palaeogeogr Palaeoclim Palaeoecol* 243:394–411
- Galfetti T, Hochuli PA, Brayard A, Bucher H, Weissert H, Vigran JO (2007c) The Smithian/Spathian boundary event: evidence for global climatic change in the wake of the end-Permian biotic crisis. *Geology* 35:291–294
- Gaston KJ (1994) *Rarity*. Chapman and Hall, London
- Gaston KJ (2000) Global patterns in biodiversity. *Nature* 405:220–227
- Gaston KJ (2003) *The structure and dynamics of geographic ranges*. Oxford University Press, Oxford
- Glenister BF, Furnish WM (1981) Permian ammonoids. In: House MR, Senior JR (eds) *The ammonoidea*. The Systematics Association, London
- Gotelli N, Colwell RK (2001) Quantifying biodiversity: procedures and pitfalls in the measurement and comparison of species richness. *Ecol Lett* 4:379–391
- Gotelli N, Colwell RK (2011) Estimating species richness. In: Magurran AE, McGill BJ (eds) *Frontiers in measuring biodiversity*. Oxford University Press, New York
- Gotelli NJ, Anderson MJ, Arita HT, Chao A, Colwell RK, Connolly SR, Currie DJ, Dunn RR, Graves GR, Green JL, Grytnes JA, Jiang YH, Jetz W, Lyons SK, McCain CM, Magurran AE, Rahbek C, Rangel T, Soberon J, Webb CO, Willig MR (2009) Patterns and causes of species richness: a general simulation model for macroecology. *Ecol Lett* 12:873–886
- Guex J, Hungerbühler A, Jenks J, O'Dogherty L, Atudorei V, Taylor DG, Bucher H, Bartolini, A (2010) Spathian (Lower Triassic) ammonoids from western USA (Idaho, California, Utah and Nevada). *Mém Géol (Lausanne)* 49:1–81
- Jablonski D, Roy K, Valentine JW (2006) Out of the Tropics: evolutionary dynamics of the latitudinal diversity gradient. *Science* 314:102–106
- Jenks J (2007) Smithian (Early Triassic) ammonoid biostratigraphy at Crittenden Springs, Elko County, Nevada and a new ammonoid from the *Meekoceras gracilitatis* Zone. *New Mexico Mus Nat Hist Sci Bull* 40:81–90
- Jenks JF, Brayard A, Brühwiler T, Bucher H (2010) New Smitian (Early Triassic) ammonoids from Crittenden Springs, Elko County, Nevada: Implications for taxonomy, biostratigraphy and biogeography. *New Mexico Mus Nat Hist Sci Bull* 48:1–41

- Jenks JF, Monnet C, Balini M, Brayard A, Meier M (2015) Biostratigraphy of Triassic ammonoids. This volume
- Klug C, Schatz W, Korn D, Reisdorf AG (2005) Morphological fluctuations of ammonoid assemblages from the Muschelkalk (middle Triassic) of the Germanic Basin indicators of their ecology, extinctions, and immigrations. *Palaeogeogr Palaeoclim Palaeoecol* 221:7–34
- Konstantinov AG (2008) Triassic ammonoids of Northeast Asia: diversity and evolutionary stages. *Stratigr Geol Correl* 16:490–502
- Konstantinov AG, Sobolev ES (2004) Specific geographic differentiation of Boreal cephalopods of Carnian age. *Russ Geol Geophys* 45:956–962
- Korn D, Ilg A (2007) AMMON. [www.wahre-staerke.com/ammon/](http://www.wahre-staerke.com/ammon/). Accessed Dec 2012
- Korn D, Titus AL, Ebbighausen V, Mapes RH, Sudar MN (2012) Early Carboniferous (Mississippian) ammonoid biogeography. *Geobios* 45:67–77
- Kummel B (1972) The Lower Triassic (Scythian) ammonoid *Otoceras*. *Bull Mus Comp Zool* 143:365–417
- Kummel B (1973a) Lower Triassic (Scythian) molluscs. In: Hallam A. (ed) *Atlas of paleobiogeography*. Elsevier, Amsterdam.
- Kummel B (1973b) Aspects of the Lower Triassic (Scythian) stage. In: Logan A, Hills LV (eds) *The Permian and the Triassic systems and their mutual boundary*. Canadian Society of Petroleum Geologists, Calgary
- Kummel B, Steele G (1962) Ammonites from the *Meekoceras gracilitatus* zone at Crittenden Spring, Elko County, Nevada. *J Paleont* 36:638–703
- Kunin WE, Gaston (1997) *The biology of rarity: causes and consequences of rare-common differences*. Chapman and Hall, London
- Legendre P, Legendre L (2012) *Numerical ecology*. Elsevier, Amsterdam
- Legendre P, Galzin R, Harmelin-Vivien ML (1997) Relating behavior to habitat: solutions to the fourth-corner problem. *Ecology* 78:547–562
- Leonova TB (2011) Permian ammonoids: biostratigraphic, biogeographical, and ecological analysis. *Pal J* 45:1206–1312
- McCain CM (2004) The mid-domain effect applied to elevational gradients: species richness of small mammals in Costa Rica. *J Biogeogr* 31:19–31
- McGowan AJ (2004) Ammonoid taxonomic and morphologic recovery patterns after the Permian–Triassic. *Geology* 32:665–668
- McGowan AJ (2005) Ammonoid recovery from the Late Permian mass extinction event. *C R Palevol* 4:517–530
- McGowan AJ, Smith AB (2007) Ammonoids across the Permian/Triassic boundary: a cladistic perspective. *Palaeontology* 50:573–590
- Monnet C, Bucher H (2005) New middle and late Anisian (Middle Triassic) ammonoid faunas from northwestern Nevada (USA): taxonomy and biochronology. *Foss Strata* 52:1–121
- Monnet C, Bucher H (2006a) Anisian (Middle Triassic) ammonoids from North America: quantitative biochronology and biodiversity. *Stratigraphy* 2:311–326 (281–296)
- Monnet C, Bucher H (2006b) Anisian ammonoids from North America: quantitative biochronology and biodiversity. *NGF Abstracts and Proceedings*, 3, 108–111
- Monnet C, Brack P, Bucher H, Rieber H (2007) Ammonite-based correlation of the middle/late Anisian boundary (Middle Triassic) between Nevada and the Southern Alps. *New Mexico Mus Nat Hist Sci Bull* 41:312–313
- Monnet C, Brack P, Bucher H, Rieber H (2008) Ammonoids of the middle/late Anisian boundary (Middle Triassic) and the transgression of the Prezzo Limestone in eastern Lombardy-Giudicarie (Italy). *Swiss J Geosci* 101:61–84
- Monnet C, Bucher H, Brayard A, Jenks JF (2013) *Globacrochordiceras* gen. nov. (Acrochordiceratidae, late early Triassic) and its significance for stress-induced evolutionary jumps in ammonoid lineages (cephalopods). *Foss Rec* 16:197–215
- Page KN (1996) Mesozoic ammonoids in space and time. In: Landman NH, Tanabe K, Davies RA (eds) *Ammonoid paleobiology*. Plenum Press, New York



- Petchey OL, Gaston KJ (2006) Functional diversity: back to basics and looking forward. *Ecol Lett* 9:741–758
- Pineda J, Caswell H (1998) Bathymetric species-diversity patterns and boundary constraints on vertical range distributions. *Deep-Sea Res II* 45:83–101
- Powell MG (2007) Latitudinal diversity gradients for brachiopod genera during late Palaeozoic time: links between climate, biogeography and evolutionary rates. *Global Ecol Biogeogr* 16:519–528
- Prim RC (1957) Shortest connection networks and some generalizations. *Bell Syst Tech J* 36:1389–1401
- Romano C, Goudemand N, Vennemann TW, Ware D, Schneebeil-Hermann E, Hochuli PA, Brühwiler T, Brinkmann W, Bucher H (2013) Climatic and biotic upheavals following the end-Permian mass extinction. *Nature Geosci* 6:57–60
- Roy K, Jablonski D, Valentine JW (2001) Climate change, species range limits and body size in marine bivalves. *Ecol Lett* 4:366–370
- Schaltegger U, Guex J, Bartolini A, Schoene B, Ovtcharova M (2008) Precise U–Pb age constraints for end-Triassic mass extinction, its correlation to volcanism and Hettangian post-extinction recovery. *Earth Planet Sci Lett* 267:266–275
- Shi GR (1993) Multivariate data analysis in palaeocology and palaeobiogeography—a review. *Palaeogeogr Palaeoclim Palaeoecol* 105:199–234
- Shigeta Y, Zakharov YD (2009) Systematic palaeontology—cephalopods. In: Shigeta Y, Zakharov YD, Maeda H, Popov AM (eds) *The Lower Triassic system in the Abrek Bay area, South Primorye, Russia*. National Museum of Nature and Science, Tokyo
- Smith EP, van Belle G (1984) Nonparametric estimation of species richness. *Biometrics* 40:119–129
- Spinosa C, Furnish WM, Glenister BF (1975) The Xenodiscidae, Permian ceratitoid ammonoids. *J Paleont* 49:239–283
- Stehli FG, Douglas RG, Newell ND (1969) Generation and maintenance of gradients in taxonomic diversity. *Science* 164:947–949
- Tozer ET (1981a) Triassic Ammonoidea: classification, evolution and relationship with Permian and Jurassic forms. In: House MR, Senior JR (eds) *The Ammonoidea*. The Systematics Association, London
- Tozer ET (1981b) Triassic Ammonoidea: geographic and stratigraphic distribution. In: House MR, Senior JR (eds) *The Ammonoidea*. The Systematics Association, London
- Tozer ET (1982) Marine Triassic faunas of North America: their significance for assessing plate and terrane movements. *Geol Rundsch* 71:1077–1104
- Tozer ET (1994) Canadian Triassic ammonoid faunas. *Geol Surv Can Bull* 467:1–663
- Urlichs M, Mundlos R (1985) Immigrations of cephalopods into the Germanic Muschelkalk basin and its influence on their suture line. In: Bayer U, Seilacher A (eds) *Sedimentary and evolutionary cycles*. Springer-Verlag, Berlin
- Villier L, Korn D (2004) Morphological disparity of ammonoids and the mark of Permian mass extinctions. *Science* 306:264–266
- Walther BA, Moore JL (2005) The concepts of bias, precision and accuracy, and their use in testing the performance of species richness estimators, with a literature review of estimator performance. *Ecography* 28:815–829
- Ware D, Jenks J, Hautmann M, Bucher H (2011) Dienerian (Early Triassic) ammonoids from the Candelaria Hills (Nevada, USA) and their significance for palaeobiogeography and palaeoceanography. *Swiss J Geosci* 104:161–181
- Zakharov YD, Moussavi Abnavi N (2013) The ammonoid recovery after the end-Permian mass extinction: evidence from the Iran-Transcaucasia area, Siberia, Primorye, and Kazakhstan. *Acta Palaeont Pol* 58:127–147
- Zakharov YD, Popov AM, Biakov AS (2008) Late Permian to Middle Triassic palaeogeographic differentiation of key ammonoid groups: evidence from the former USSR. *Polar Res* 27:441–468
- Zhang Y, Payne JL (2012) Size-frequency distributions along a latitudinal gradient in Middle Permian fusulinoideans. *Plos One* 7:e38603